Two mechanisms of the negative-effective-mass instability in *p*-type quantum well-based ballistic p^+pp^+ -diodes: Simulations with a load

R. R. Bashirov, Z. S. Gribnikov,^{a)} N. Z. Vagidov, and V. V. Mitin Department of Electrical and Computer Engineering, Wayne State University, Detroit, Michigan 48202

Department of Decenteur and comparer Distincering, wayne office on tersity, Deron, mengan

(Received 21 August 2000; accepted for publication 9 October 2000)

There exist two regimes of the negative-effective-mass (NEM) instability in ballistic p^+pp^+ -diodes with two-dimensional hole gas in the *p*-base: the instability of homogeneous NEM-hole distribution in a quasineutral plasma region, and the instability of a thin accumulation layer, which forms inside a depletion region and contains NEM holes. Both instabilities lead to the development of terahertz oscillatory regimes. The regimes' simulation in the inductance-loaded diodes with base lengths 0.05–0.15 μ m demonstrates that such loads substantially enlarge the voltage range of the second regime and give rise to oscillatory regimes, which do not appear in unloaded diodes at all. Efficiencies of different oscillatory regimes are estimated. © 2000 American Institute of Physics. [S0003-6951(00)00250-3]

This letter is devoted to simulation of terahertz oscillatory regimes in ballistic p^+pp^+ -diodes with short-channel p-bases. We assume that these bases can be grown in the form of narrow (8 nm wide) p-type quantum wells (p-QWs) on (311) A-GaAs substrates (in the GaAs/AlGaAs system). It is known, that such *p*-QWs have extremely high values of low-temperature mobility for narrow wells and *p*-type materials (see Refs. 1 and 2 and also Ref. 3 as a review). This allows us to plan sufficiently long mean free paths of holes in the bases. It is also known,^{1,4,5} that a hole dispersion relation $\epsilon(p)$ (where p is a momentum) contains a negative-effectivemass (NEM) section around some momentum value p $= p_C$, for a ground quantization state in a symmetric p-QW (see Fig. 1(a), where a velocity $v(p) = d\epsilon(p)/dp$ is also shown). We assume [Fig. 1(b)] that the *p*-GaAs QW channels form a periodic structure (with space periods a=0.04 μ m) enclosed between p^+ -emitter (source) and p^+ -collector (drain) contact planes, spatially distanced by a base length, l $(l=0.15, 0.10, 0.08, 0.065, 0.060, and 0.055 \ \mu m)$. The nonconducting AlAs barriers (containing acceptor sheets of modulation doping) isolate the channels from each other. These diodes are electrically loaded with inductance L, which varies in a range from 0 to several pH cm.

All of the simulated NEM diodes demonstrate terahertz oscillatory regimes (ORs). Such regimes are displayed for diodes with l=0.15, 0.10, and 0.08 μ m at L=0. The diodes with $l \leq 0.065 \mu$ m need a certain minimal inductance $L_m(l)$ to reveal ORs. These ORs can be substantially modified as a result of L variations from 0 [or $L_m(l)$] to some maximal value $L_M(l)$, when the oscillatory regime disappears entirely. As it is first noted in Ref. 3, two different limiting ORs occur in ballistic NEM diodes. The first, OR1, takes place for comparatively small voltages across a diode (in the investigated diodes $\sim 15-35$ mV). This segment corresponds to unstable current saturation section [V_C , V_K] in a stationary J-V characteristic [Fig. 1(c)]. The second, OR2, occurs for higher voltages ($V > V_K$, really V > 35-40 mV) where the

saturation section of the unstable stationary J-V characteristic gives way to an increasing current branch. This section of OR2 has no clear (determined in advance) upper voltage limit. It depends on the base length *l*, the load inductance *L*, etc. As a rule oscillation frequencies in OR2 are noticeably higher than in OR1. Oscillation current amplitudes in OR2 are also substantially larger than in OR1, if the OR2 section is well developed.

Envelopes of oscillation portraits for the diode with $l=0.08 \ \mu\text{m}$ at L=0 and at six values of L are presented in Fig. 2. We see that at L=0 oscillations take place in a very short voltage interval in the current saturation section (that is, they are of OR1). At L=0.005 pH cm, the voltage segment of oscillations extends, and beginning with L=0.0095 pH cm, it includes some voltage interval at $V>V_K$, meaning we have also induced oscillation activity in OR2. The maximal oscillation activity in OR2 occurs around L=0.013

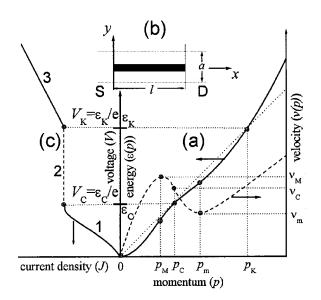


FIG. 1. (a) The dispersion relation $\epsilon(p)$ and the velocity $v(p) = d\epsilon(p)/dp$ used for our simulation. (b) Design of the simulated device cell. (c) The unstable stationary J-V characteristic: (1) the stable small current branch; (2) the unstable current saturation section; (3) the branch of increasing current (with the possible accumulation layer instability).

3785

© 2000 American Institute of Physics

Downloaded 29 Sep 2003 to 128.205.55.69. Redistribution subject to AIP license or copyright, see http://ojps.aip.org/aplo/aplcr.jsp

^{a)}Electronic mail: zinovi@besm6.eng.wayne.edu

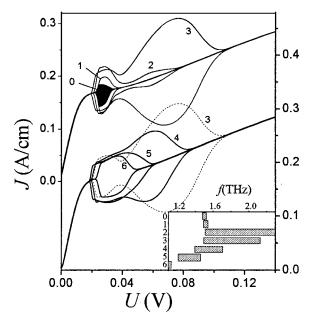


FIG. 2. J-V characteristic and envelopes of current oscillation portraits for $l=0.08 \ \mu\text{m}$ at different inductance loads L (pH cm): (0) 0; (1) 0.005; (2) 0.0095; (3) 0.013; (4) 0.027; (5) 0.040; (6) 0.066. In the inset: oscillation frequency ranges for the same cases 0-6.

pH cm. Further increases in L lead to some increase in OR1 and to fast suppression of OR2. Beginning with L=0.040pH cm, increase in L causes only gradual suppression of oscillation activity up to its disappearance. Oscillation amplitudes behave nonmonotonically with a monotonic increase in L: they increase, reach maximal values, and collapse to zero. But rates of frequency and amplitude variations substantially differ for these ORs: OR2 reacts to inductance variations with far greater rates than OR1. Oscillation amplitude in OR2 and the voltage interval for this regime both increase very fast with an increase in L, and then quickly decrease. Corresponding variations of oscillation amplitudes for QR1 are much slower. Continuous variations of oscillation activity in the same diode at two voltage values (V=30 and 60 mV) induced by changing L(t) are depicted in Fig. 3. We observe pictures of primary development and subsequent suppression of oscillatory activity both in the OR1 and in the OR2 sections. Note that in Fig. 2 we operate with voltages V(t), which only rise with time. All of the transitions from nonoscillating states to ORs considered here are abrupt (similar to the nonequilibrium phase transitions of the first kind). This means that we must obtain certain hysteretic phenomena: other (smaller) values of critical voltages $V_{C,K}$ and inductances $L_{m,M}(l)$ for back direction of variations V(t)and L(t). We can observe such hysteretic phenomena in Fig. 3, where envelopes of oscillation portraits are shown for both directions of the L(t) variations. The hysteresis explains some contradictions between Figs. 2 and 3. In the shortest base diodes ($l \le 0.065$ m) there are no oscillations at L=0. They appear beginning with some $L_m(l)$. The shorter diode base is, the less OR2 is pronounced. As a result of disappearance of OR2 in the shortest base diodes, we cannot reach frequencies higher than 2.2-2.3 THz for the considered diode family.

The two ORs demonstrating different behaviors depend-

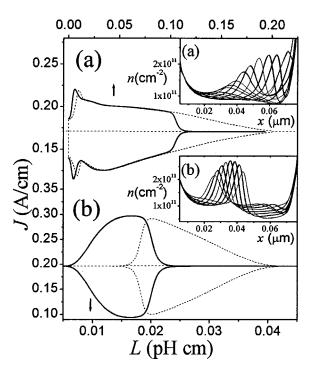


FIG. 3. Envelopes of current oscillation portraits for the same example as in Fig. 2 at V=30 mV (a) and V=60 mV (b) for increasing with time t (dotted curves) and decreasing (solid curves) load inductances L(t). In inset (a) snapshots of hole concentration distribution in the diode base at V=30 mV and L=0.013 pH cm. In inset (b) the same at V=60 mV and L=0.013 pH cm. Asymmetry of the envelopes for small values of the L(t) at V=30 mV is connected with substantial nonlinearity of current oscillations.

different physical origin. OR1 forms as a result of the development and globalization of classic convective instability⁶ occurring in a quasineutral NEM-plasma region. The unstable solution of the corresponding stationary problem leads to a NEM-plasma region between a source-adjacent spatialcharge region (SSCR) and a drain-adjacent SCR (DSCR) in the voltage section (V_C, V_K) in Fig. 1(c). The voltage part V_C drops across the SSCR, and the rest, $V-V_C$, drops across the DSCR ($V \le V_K$). A global instability of this stationary solution leads to the development of an oscillatory regime. Nuclei of spatial charge waves appear in the SSCR and develop, shifting to the quasineutral region and transforming into dipole domains (with an extended depletion layer and a much narrower accumulation layer). A voltage, which drops across such domain, increases with the domain's movement and development. Since this voltage $V_D(t)$ depends on time, a remaining voltage across the SSCR, V $-V_D(t)$, also depends on time. Therefore, the height of the effective "anode" determined by this voltage and an emitted current determined by this height also depend on time. Current oscillations appear and initiate appearance of new spatial-charge wave nuclei. In this scenario, the maximal development of the above-described moving waves and domains takes place on the right side of the base near the drain [see inset (a) in Fig. 3]. This scenario loses its vigor at V nearing V_K because then the structure of the unstable stationary solution changes substantially. At $V \ge V_K$ such stationary solution contains neither the quasineutral NEM-plasma region nor obviously pronounced DSCR. NEM holes are now found only in an accumulation layer pulled into the SSCR.

ing on voltage and inductance load variations are of some The latter becomes much wider because almost all the volt-Downloaded 29 Sep 2003 to 128.205.55.69. Redistribution subject to AIP license or copyright, see http://ojps.aip.org/aplo/aplcr.jsp age V, which is now much higher than V_C , drops across this new SSCR (with the accumulation layer inside the SSCR). The quasineutral region (if existing) is now not occupied by NEM holes. Nevertheless, it turns out that the presence of the above-mentioned accumulation layer (with its left slope occupied by NEM holes) is sufficient to induce a global instability and OR2 in the diode. But a route of spatial-charge waves is much shorter at OR2 than in the case of OR1. These waves are now concentrated around the unstable stationary position of the accumulation layer inside the SSCR [see inset (b) in Fig. 3]. With an increase in the voltage V, this position shifts to the source more and more. Such waves include accumulation layers that are noticeably narrower than the unstable stationary accumulation layer. They redistribute electric fields in the entire SSCR and lead to oscillations of the effective anode height (as above in case of OR1) and to source-emitted current oscillations.

At least in the longer-base diodes (for example, at $l=0.15 \ \mu$ m), these oscillations of the spatial charge and emitted current induce two-stream oscillations in the drainadjacent quasineutral section of the base. In contrast to spatial-charge waves, the two-stream oscillations are almost quasineutral. To clarify these oscillations we have considered different p_x cross sections of a hole distribution function $F(p_x, x, t)$ for $p_z=0$. As it is known,⁷⁻¹⁰ the two-stream instability in ballistic diodes can itself lead to terahertz oscillatory regimes (without any NEM dispersion). It seems possible that the displayed two-stream oscillations gain OR2 in the longer-base diodes.

Along with the influence of inductive loads we also consider the effect of active loads on oscillatory regimes. Naturally, increasing active load resistance R monotonically decreases amplitude of generated current oscillations. But the oscillation power released in the load, $W = \langle J^2 R \rangle$, reaches a certain maximal value $W = W_0$ at an optimal value $R = R_0$. For the diode with $l=0.15 \ \mu m$ we obtain $R_0=0.48 \ \Omega \ cm$ and $W_0 = 0.1165$ mW/cm for the operating voltage across diode $V = V_0 = 60$ mV and the mean current $\overline{J} = J_0 = 0.174$ A/cm. The efficiency for these numbers is $\eta \approx 0.47\%$. It can be increased noticeably by selecting an optimal inductance. We have used the following technique to simplify calculations of oscillatory regimes in the loaded diodes. Nonstationary current J(t) in each cross section x is determined by the sum of the convective current $J_C(x,t)$, which is carried by channel holes, and the displacement current. The latter is formed by a longitudinal component of alternating electric field $E_X(x,y,t)$ in all the spaces between the source and drain. It can be simply shown that for the simulated planeparallel diode design $J(t) = C(dV/dt) + \overline{J}_C(t)$, where $\overline{J}_C(t)$ $=(1/l)\int_0^l J_C(x,t)dx$, and C is the constant drain-source capacity for a single cell of the selected periodic system [Fig.

1(b)]: $C = \kappa_D a/4\pi l$, and κ_D is a dielectric constant. If the diode is connected in series to active resistance *R*, inductance *L*, and power supply with electromotive force *U* we obtain V = U - J(t)R - L(dJ/dt) and $J(t) = \overline{J}_C(t) - CR(dJ/dt) - CL(d^2J/dt^2)$. The described scheme is convenient because only capacity *C* and the convective current represent the diode. The latter must be homogeneously averaged for any moment *t*.

In conclusion, we have shown that the two limiting mechanisms of NEM terahertz generation lead to substantially different reactions to inductance loads. Such loads have a much greater influence on the higher-voltage OR2. Specially selected inductance loads allow oscillatory regimes in very short base diodes (with *l* up to 0.05 μ m and may be shorter). For such short base lengths and for low temperatures (≤ 20 K), we can expect for realistic ballistic hole transport in *p*-type QWs grown on $\langle 311 \rangle$ A–GaAs substrates as well as in multilayer systems of these QWs. Analogous expectations can be related to multilayer ΓX -GaAs/AlGaAs QW systems with an NEM-electron generation mechanism.¹¹ The suggested NEM generators promise comparatively high efficiencies (in comparison with most other terahertz sources, including both real and proposed ones).

The authors cordially thank Professor G. Haddad from University of Michigan for numerous stimulating discussions and O. Melnikova from the same university for valuable help. This work is supported by the NSF grant.

- ¹B. E. Cole, J. M. Chamberlain, M. Henini, T. Cheng, W. Batty, A. Wittlin, J. A. A. J. Perenboom, A. Ardavan, A. Polisski, and J. Singleton, Phys. Rev. B 55, 2503 (1997).
- ²B. R. Perkins, J. Liu, A. Zaslavsky, Z. S. Gribnikov, V. V. Mitin, E. P. De Portere, and M. Shayegan, *Proceedings of the 11th International Symposium on Space Terahertz Technology* (University of Michigan, Ann Arbor, MI, 2000), p. 573.
- ³Z. S. Gribnikov, A. N. Korshak, and V. V. Mitin, Int. J. Infrared Millim. Waves **20**, 213 (1999).
- ⁴R. K. Hayden, D. K. Maude, L. Eaves, E. C. Valadares, M. Henini, F. W. Sheard, O. H. Hughes, J. C. Portal, and L. Cury, Phys. Rev. Lett. **66**, 1749 (1991).
- ⁵R. K. Hayden, L. Eaves, M. Henini, E. C. Valadares, O. Kuhn, D. K. Maude, J. C. Portal, T. Takamasu, N. Miura, and U. Ekenberg, Semicond. Sci. Technol. 9, 298 (1994).
- ⁶E. M. Lifshitz and L. P. Pitaevski, *Physical Kinetics* (Pergamon, Oxford, 1980).
- ⁷N. A. Bannov, V. I. Ryzhii, and V. A. Fedirko, Sov. Phys. Semicond. **17**, 36 (1983).
- ⁸V. I. Ryzhii, N. A. Bannov, and V. A. Fedirko, Sov. Phys. Semicond. 18, 481 (1984).
- ⁹Z. S. Gribnikov, N. Z. Vagidov, A. N. Korshak, and V. V. Mitin, J. Appl. Phys. **87**, 7466 (2000).
- ¹⁰Z. S. Gribnikov, N. Z. Vagidov, and V. V. Mitin, J. Appl. Phys. 88, 6736 (2000).
- ¹¹Z. S. Gribnikov, A. N. Korshak, and N. Z. Vagidov, J. Appl. Phys. 80, 5799 (1996).